NUMERICAL MODELING OF THE COMPRESSION PROCESS IN SCROLL COMPRESSORS

Evandro L. L. Pereira, evandro.l.l.pereira@gmail.com
Cesar J. Deschamps, deschamps@polo.ufsc.br
POLO – Research Laboratories for Emerging Technologies in Cooling and Thermophysics
Department of Mechanical Engineering
Federal University of Santa Catarina
88040-900, Florianópolis, SC, Brazil

Abstract. *Scroll compressors are positive-displacement machines that compress a mass of gas through the relative orbital motion between two interfering spiral-shaped scroll members. Such compressors are usually found in high capacity HVAC applications, such as air-conditioning and water heating, and known for their efficiency, reliability, quiet operation and low vibration. The internal gas leakage and the suction gas superheating are the main source of inefficiency in scroll compressors. This paper presents a numerical model to simulate the compression process of a scroll compressor, based on a lumped formulation for mass and energy conservation equations. The refrigerant mass flow rate thorugh suction and discharge valves are calculated with reference to an isentropic flow condition, whereas the internal gas leakages are estimated from a quasi-1D model that includes viscous and convective effects. A one-degree of freedom model is used to describe the discharge valve dynamics. A real gas equation of state closes the set of equations. The model is applied to investigate the performance of a scroll compressor under different operating conditions and design changes.*

Keywords*: refrigeration, scroll compressor, numerical simulation*

1. INTRODUCTION

According to ASHRAE (2004), the scroll compressor is a positive displacement and orbital motion machine, which performs the process of compression by two interfitting, spiral-shaped scroll members. The concept of the scroll compressor is not new, though it can be regarded as a relatively recent technology. In fact, the concept was patented in 1905 by French engineer Léon Creux, initially as a expanding vapor device (CREUX, 1905). Although its potential as a vapor compressor has been identified long ago (Ekelöf, 1933), only in the mid-1970s the manufacturing process achieved a sufficient level of development for which a prototype could be built. The scroll compressor was originally manufactured in Japan and the United States, and the technology finally spread to the refrigeration and HVAC applications in the mid-1980s. Today, the scroll compressor can be found in many residential and commercial applications. Continued research and development of scroll technology has made it possible to manufacture single units with capacities of up to 25 tons. Nevertheless, compressor sets with two, three and four compressors makes it possible to successfully apply scroll compressors in chillers with total capacities approaching 300 tons (CARRIER, 2004).

A scroll compressor consists of two elements in the form of a spiral of identical geometry, mounted inverted and rotated 180º from one to the other (Fig. 1). When assembled, the flanks of the orbiting and stationary scroll vanes form crescent-shaped pockets. As the scroll orbits, the sealing points (tangent lines) on the vane flanks migrate inward, pushing the pockets toward the involute center. As the pockets move, they decrease in volume and consequently compress the trapped gas. Figure 2 shows a sequence of orbits, from which one can observe the movement and variation of the trapped gas pockets.

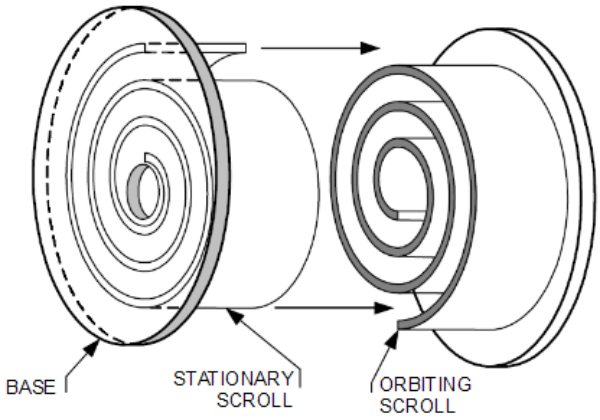

Figure 1. Schematic representation of a scroll set; reproduced from CARRIER (2004).

At the orbital angle $\theta = 0^{o}$, the suction pocket begins to be formed outside of the spiral. As the scroll orbits, the volume of the suction pocket increases and gas is admitted from the suction line, as shown in Fig. 2(a). The contact between the tip of the orbiting scroll vane against the stationary scroll vane occurs after a complete revolution, sealing the suction pocket and starting the compression process of the trapped gas (Fig. 2(b)). In the compression chambers, the gas is compressed while transported toward the central region of the compressor, as indicated by Figures 2(c)-(d). At a certain point, the pockets symmetrically opposed meet each other at the discharge region, creating a new single pocket (Figure 2(e)) and starting the discharge process. The angle in which the discharge region is formed depends on the geometry of the spiral curves and is frequently referred to as discharge angle. As the process progresses (Figure 2(f)), the refrigerant gas is eventually released through the discharge port, properly positioned in the center of the stationary scroll. It should be noted that throughout the operation of the compressor, all pockets are filled with gas and, therefore, the compression process occurs in a continuous way.

(a) 180° (Suction) (b) 360° (End of suction process and beginning of compression process) (c) 540° (Compression)

(d) 720° (Compression) (e) 900° (Beginning of discharge) (f) 1170° (Discharge)

Figure 2. Compression process; adapted from Gomes (2006).

The scroll compressor is well-known by its efficiency in applications that demand high refrigeration capacities. In low capacity applications, it is usually applied in air conditioning systems, application in which the compression ratio is lower. An advantage inherent to the scroll compressor in comparison to other mechanisms of compression is the absence of valves and the time available for the processes of suction and discharge. Other benefits offered by scroll compressors are high volumetric efficiency (close to 100% for air conditioning and heat pump applications), low vibration, very quite operation and few moving parts. Among its main sources of thermodynamic irreversibility, pressure equalization at the beginning of the discharge process and internal gas leakages stand out. The losses originated by the former is usually diminished or eliminated by using valves. The later has been a constant concern in the design of scroll compressors, since it is responsible for low efficiency of scroll compressors in applications with high compression ratio.

There are two different paths for the internal gas leakage between two adjacent pockets in a scroll compressor (Fig. 3). The first one is formed by the gap between the top of a scroll and the base of the other (top clearance). This type of leakage is called top leakage or radial leakage. The other leakage path is formed by the clearance between the flanks of two scroll vanes (flank clearance) and it is called flank leakage or tangential leakage. Besides degrading the volumetric efficiency, leakages also reduce the isentropic efficiency, since an extra amount of energy is required to re-compress the mass of gas that leaked.

The first numerical methodology to simulate a scroll compressor was presented by Morishita *et al.* (1984), in which the compression process was modeled via a lumped formulation. The model developed by Morishita *et al.* (1984) served as basis for the development of several other simulation methodologies (Tojo *et al.*, 1986; Caillat *et al.*, 1988; Nieter, 1988; Yanagisawa *et al.*, 1990; Suefuji *et al.*, 1992; Chen *et al.*, 2002). Among all models that adopt a lumped formulation, the one described by Chen *et al.* (2002) can be considered the most comprehensive. In such models,

different approaches are employed to predict the gas leakage, becoming clear that there some uncertainty about the most appropriate one. In spite of that, it seems the modeling of leakage with reference to an isentropic flow in nozzles is the most widespread, with the viscous effects being included by means of contraction flow factors.

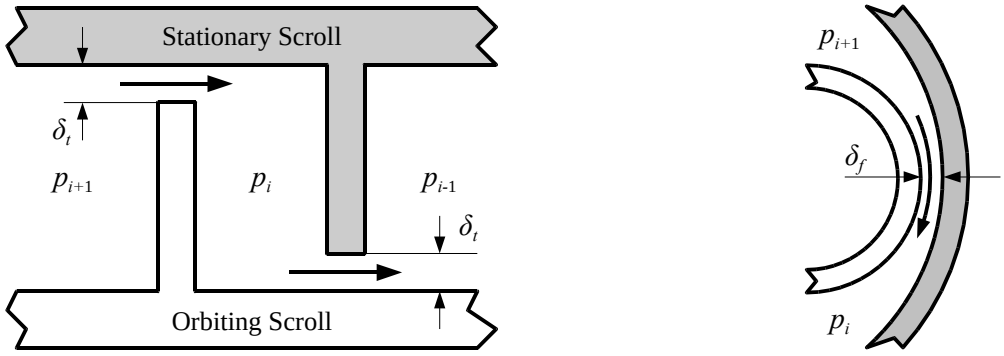

(a) Top leakage. (b) Flank leakage.

Figure 3. Paths for the internal leakages in a scroll compressor.

This paper presents a numerical model developed to simulate the compression process of a scroll compressor. The mass and energy conservation equations are solved using a lumped formulation. An appropriated real gas equation of state is adopted by means of libraries provided in the code REFPROP (NIST, 2008). Mass flow rates through suction and discharge valves, as well as leakage in flank clearances, are calculated from relationships based on the isentropic flow condition. Unlike most models described in the literature, a quasi-1D model that includes viscous and convective effects is used to predict the gas flow through the top clearance. A one-degree of freedom model is used to describe the discharge valve dynamics. The model is applied to investigate the performance of a scroll compressor for different operating conditions and design alternatives.

2. MATHEMATICAL MODEL

2.1 Geometric Definitions

The shape of the scroll here modeled is an involute of a circle. The scroll is consequently defined by two involutes that develop around a common basic circle of radius a and are offset by a constant distance r_o. From the definition of the involute, the distance L of one point on the involute to its tangent point on the base circle must satisfy the following mathematical relationship:

$$\frac{\partial L(\varphi)}{\partial \varphi} = a \tag{1}$$

where φ is the involute angle. For a scroll with N compression chambers, φ varies from the initial involute angle α to the involute ending angle φ_e ($\varphi_e = 2\pi N + \pi/2$). Therefore, by integrating Eq. (1) and assuming a is a constant, the equations describing the pair of involutes in polar coordinates can be obtained (Chen *et al*., 2002). From these relationships, the scroll vane thickness t, the orbiting radius of the rotating scroll r_o and the displacement volume V_{sw} can be written as follows:

$$t = 2a\alpha \tag{2}$$

$$r_o = a\pi - t \tag{3}$$

$$V_{sw} = 4\pi^2 a(\pi a - t)(2N - 1)h \tag{4}$$

where h is the scroll vane height.

The central region of the scroll can be designed with different geometric shapes. In this work, the profile of the scrolls in the central region is constructed from the geometric and mathematical description given by Zhenquan *et al*. (1992), which is a function of a modified angle γ and an angle β that must satisfy the following relationship:

$$\text{ctg}\,\beta + 2\beta = \pi + \gamma \tag{5}$$

Therefore, the discharge angle θ_d and the maximum discharge radius r_d for a circular port are calculated by:

$$\theta_d = 2\pi N - \gamma \tag{6}$$

$$r_d = \frac{a}{\text{sen}(2\beta)} - \frac{r_o}{2} \tag{7}$$

Furthermore, the suction area A_s, the flank leakage area A_f and the top leakage area A_t can be calculated by the following expressions:

$$A_s = hr_o\left[1-\cos(\theta)\right] + h\delta_f \tag{8}$$

$$A_f = h\delta_f \tag{9}$$

$$A_t = \delta_t \int_{\varphi_1}^{\varphi_2} L\,\mathrm{d}\varphi = \delta_t a\left(\varphi_2^2 - \varphi_1^2\right) \tag{10}$$

where δ_f and δ_t are the flank clearance and the top clearance, respectively, and φ_1 and φ_2 are integral limits listed in Tab. 1.

Table 1. Integral limits to calculate the top leakage area.

Orbiting angle	φ_1	φ_2
$2\pi \le \theta \le 3\pi$	$\varphi_e - \alpha_i + \pi - \theta$	$\varphi_e - \alpha_i - \pi$
$3\pi \le \theta \le 2\pi + \theta_d$	$\varphi_e - \alpha_i + \pi - \theta$	$\varphi_e - \alpha_i + 2\pi - \theta$

Due to the shape of the scroll central region, an error arises when one evaluates the volume of the compression chambers by using the mathematical expressions available in the literature (Chen *et al.*, 2002; Wang *et al*., 2005). Thus, such volumes were calculated in the present study through the integration of parametric functions, which define the involutes curves of the stationary and the orbiting scrolls vanes. Due to space limitations, the resulting expressions will not be presented in this paper.

2.2 Compression process

As mentioned before, the numerical model developed in the present work adopted a lumped formulation. Hence, time variations of temperature *T*, mass *m* and pressure *p* in a certain volume of gas can be calculated from equations for conservation of mass and energy:

$$\frac{\partial m}{\partial t} = \sum \dot{m}_{in} - \sum \dot{m}_{out} \tag{11}$$

$$\frac{\partial T}{\partial t} = \frac{1}{mc_v}\left\{-T\left(\frac{\partial p}{\partial T}\right)_V\left[\frac{\partial V}{\partial t} - \frac{\left(\sum \dot{m}_{in} - \sum \dot{m}_{out}\right)}{\rho}\right] - \sum \dot{m}_{in}\left(h - h_{in}\right) + \dot{Q}\right\} \tag{12}$$

Equations (11) and (12) are solved by the Euler's method. The third equation required to determine the thermodynamic properties of the gas is an equation of state. In this work, this task was accomplished through a link to the code REFPROP (NIST, 2008). Heat transfer between the gas and the scroll walls was not considered at this point.

The mass flows rates regarding to the processes of suction, discharge and flank leakage are estimated by the following equation for isentropic flows, corrected by a contraction flow coefficient, C_c:

$$\dot{m} = C_c A\sqrt{2p_h\rho_h}\sqrt{\frac{\gamma}{\gamma-1}\left[\left(\frac{p_l}{p_h}\right)^{\frac{2}{\gamma}} - \left(\frac{p_l}{p_h}\right)^{\frac{\gamma+1}{\gamma}}\right]} \tag{13}$$

On the hand, leakage through the top clearance is predicted by a quasi-1D model, as described by Huang (1994):

$$\frac{\delta^4(\gamma-1)\mu}{80\gamma p}G^3+\frac{1}{120}\left(\delta^3\frac{d\delta}{dx}+\frac{\delta^4}{\gamma p}\frac{dp}{dx}\right)G^2+\frac{\mu}{\rho}G-\frac{1}{\rho}\frac{dp}{dx}=0 \tag{14}$$

$$\dot{m}=-\frac{\rho\delta^3}{12}G \tag{15}$$

In Eq. (13), a contraction flow coefficient C_c of 0.7 was adopted for all processes. As the model of Huang (1994) already includes viscous effects and geometric variations, there is no need for specifying a contraction flow coefficient in Eq. (15).

In any situation, the pressure ratio is limited by the chocked flow condition:

$$\left(\frac{p_l}{p_h}\right)_{\text{critic}}=\left(\frac{2}{\gamma+1}\right)^{\frac{\gamma}{\gamma-1}} \tag{16}$$

Unlike the usual procedure of simulating the compression in all pockets simultaneously, the methodology adopted here follows a pocket from the beginning of the suction process to the end of the discharge process. Thus, for the first compression cycle gas properties in the posterior pocket (closer to the central region) are unknown and only the internal gas leakage leaving the pocket is really calculated. Then, during the simulation of a new compression cycle, the mass of gas entering the pocket due to gas leakage assumed to be equal to the amount leaked out the pocket in the previous cycle, as outlined in Fig. 4. Besides reducing the number of calculations, this approach acts as an under-relaxation factor, returning a greater numerical stability to the iterative solution procedure. The convergence of the numerical solution is checked by monitoring the mass unbalance and cyclical variations in the discharge temperature.

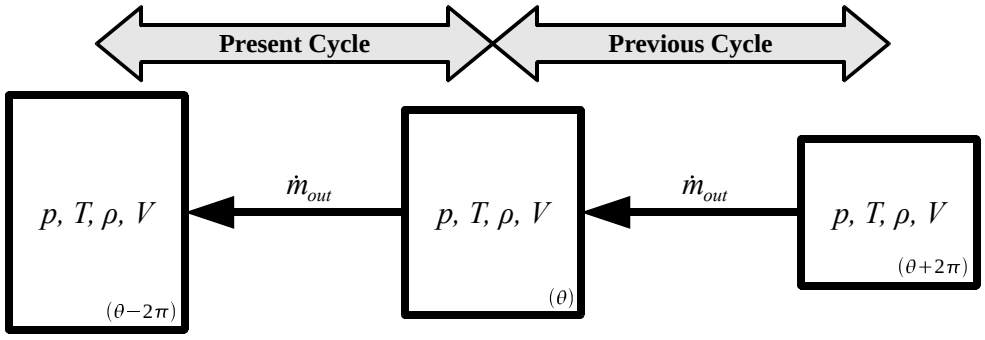

Figure 4. Schematic representation of the numerical procedure to evaluate internal gas leakages.

3. RESULTS AND DISCUSSION

The geometric parameters and the operating conditions used to establish a reference case for other simulations are listed in Tab. 2 and Tab. 3, respectively. By default, the compressor does not employ a discharge valve, but its use is discussed. A time step equivalent to a crankshaft angle of 0.05º was adopted in all simulations.

Figures 5-8 presents the influence of the evaporation and condensation temperatures on the compressor performance in terms of cooling capacity, power consumption, discharge temperature and isentropic efficiency. The mass flow rate remains virtually the same for different evaporation temperatures. Hence, the cooling capacity only changes with the condensation temperature, as Fig. 5 shows. As expected, the power consumption indicated in Fig. 6 is seen to increase with the condensation temperature, due to the higher compression ratio. Despite the presence of leakage effects, one can demonstrate that the discharge temperature and the isentropic efficiency are more influenced by the pressure equalization process. Basically, there is a trend for the scroll compressor to present a higher isentropic efficiency when subjected to a compression ratio closer to that imposed by its built-in volume ratio. This can be easily understood from Figs. 9 and 10, which shows respectively p-V and T-V diagrams for a condensation temperature T_c = 45ºC. For the evaporation temperature T_e = -10ºC, the compression ratio associated with the system is very close to that imposed by the compressor built-in volume ratio at the discharge angle, resulting in a high isentropic efficiency. On the other hand, when the evaporation temperature is either decreased to T_e = -30ºC or increased to T_e = 10ºC, there is

decrease in the isentropic efficiency due to under and over compression losses, respectively. The negative effect of under compression can be reduced through the use of discharge valves. As Fig. 6 shows, the adoption of a discharge valve increases the isentropic efficiency from 74.2% to 81.6%, whereas the discharge temperature was decreased from 78.4ºC to 73.4ºC. On the other hand, over compression losses can only be reduced through the incorporation of valves at intermediate positions of the scroll.

Table 2. Geometric parameters for the reference scroll compressor.

Parameter	Variable	Value
Radius of the basic circle [mm]	a	2.0
Wrap thickness [mm]	t	3.0
Displacement volume [cm³]	V_{sw}	2 x 10.0
Number of compression chambers	N	3
Modified angle [degrees]	γ	60.0
Top clearance [μm]	δ_t	5.0
Flank clearance [μm]	δ_f	10.0

Table 3. Reference operating conditions.

Parameter	Variable	Value
Nominal frequency of operation [rpm]	F	3000.0
Refrigerant fluid	-	R404a
Temperature of evaporation [ºC]	T_e	-10.0
Temperature of condensation [ºC]	T_c	45.0
Subcooling [ºC]	ΔT_c	0.0
Superheating [ºC]	ΔT_h	10.0
Temperature of suction [ºC]	T_s	$T_e + \Delta T_h$

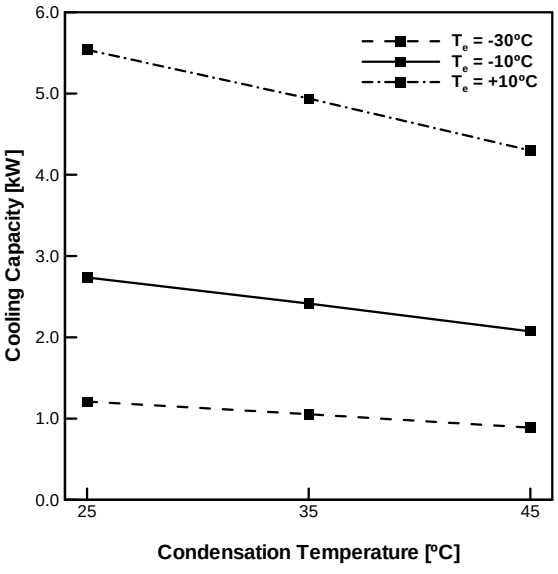

Figure 5. Influence of operating condition on the cooling capacity.

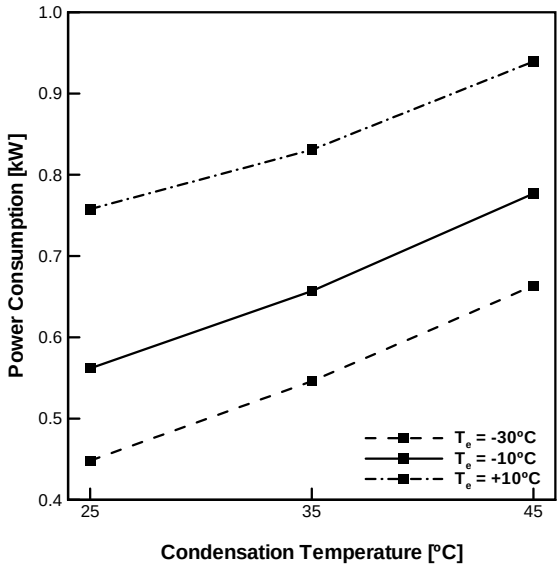

Figure 6. Influence of operating condition on the power consumption.

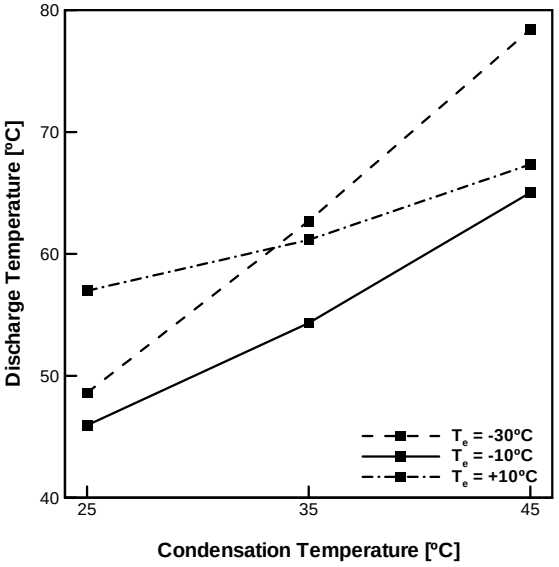

Figure 7. Influence of operating condition on the discharge temperature.

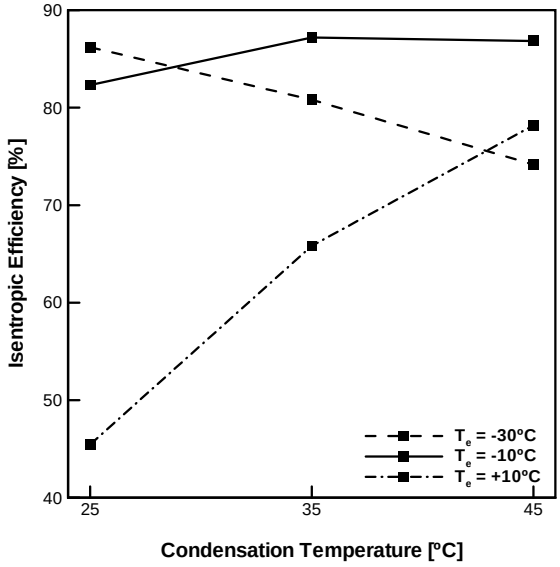

Figure 8. Influence of operating condition on the isentropic efficiency.

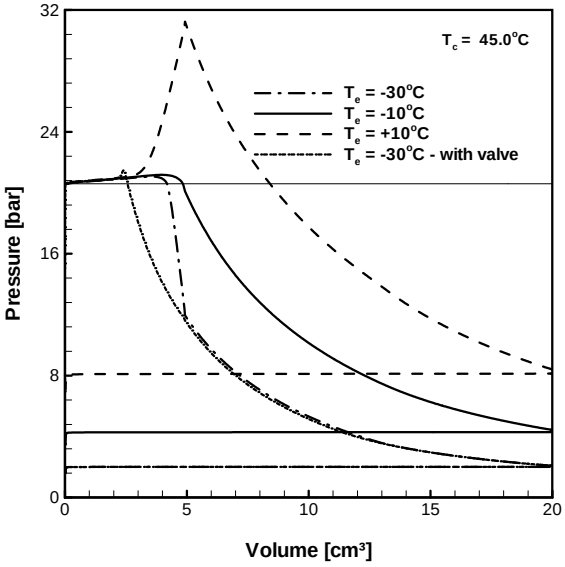

Figure 9. Result for p-V considering a condensation temperature of 45ºC.

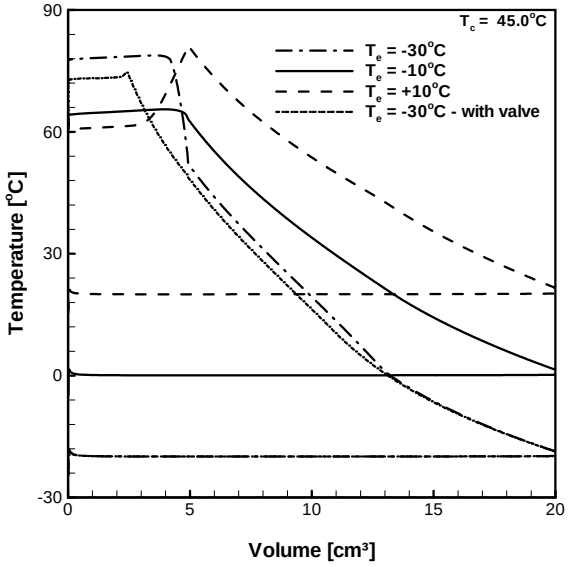

Figure 10. Result for T-V considering a condensation temperature of 45ºC.

The impact of internal leakages on the scroll compressor is presented in Figs. 11-14, based on results from simulations for T_e = -10ºC and T_c = 35ºC, by varying the clearances from 5 to 20 µm. For clarity, top and flank leakages were separately analyzed. Overall, it is clear that the top leakage has a stronger impact on the compressor performance than the flank leakage due to its larger leakage areas. Figure 11 shows the associated drop in the mass flow rate when the top and flank clearances are increased. The effect of the internal gas leakage on the volumetric efficiency is directly proportional to the mass flow rate. The reduction of power consumption observed when the top clearance is changed to 20 µm (Fig 12) is a consequence of the smaller amount of mass that is compressed. The mass of gas that leaks from a higher pressure pocket to a lower pressure pocket requires an extra quantity of energy to be re-compressed, degrading the compressor isentropic efficiency (Fig 14). Moreover, the gas temperature in the lower pressure pocket is also raised, increasing the discharge temperature (Fig 13).

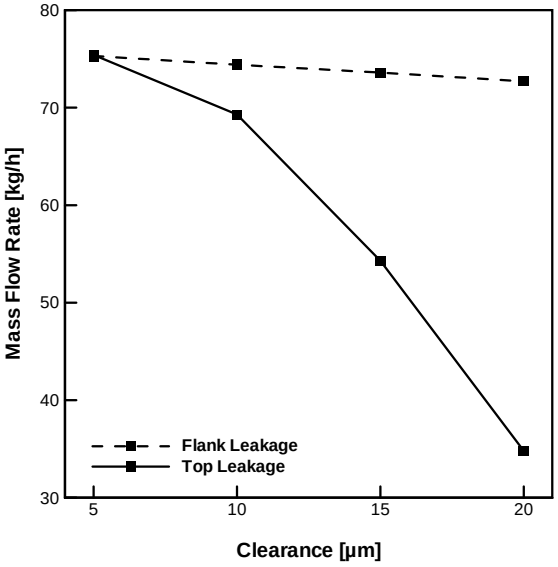

Figure 11. Impact of internal leakage on the mass flow rate.

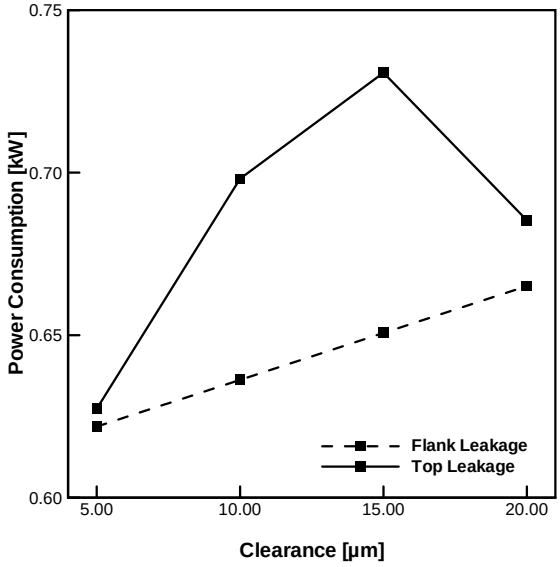

Figure 12. Impact of internal leakage on the power consumption.

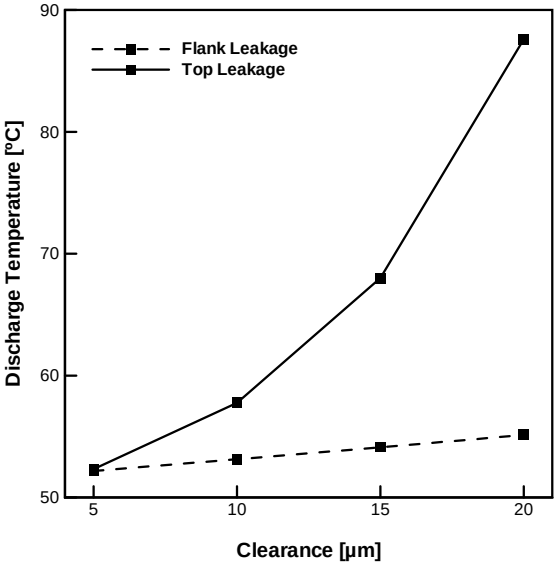

Figure 13. Impact of internal leakage on the discharge temperature.

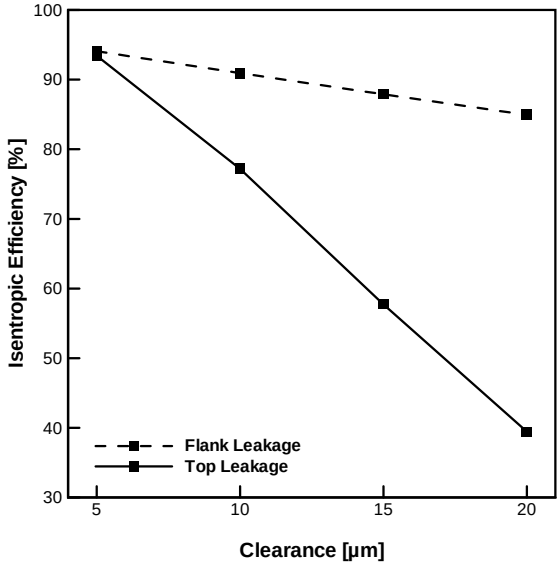

Figure 14. Impact of internal leakage on the isentropic efficiency.

In order to analyze the influence of geometric parameters on the compressor performance, the radius of the basic circle a was varied. The height of the wraps was changed for each radius so as to maintain the compressor displacement V_{sw}. The discharge port diameter was changed to reach the maximum value for the geometry in study. The other geometric parameters were kept constants. Essentially, the increase of the basic circle increases the length of the top clearance, therefore increasing the top leakage. On the other hand, to keep the same displacement volume, the height of the wraps has to be reduced, bringing about a decrease in the flank leakage. For the compressor and the operating conditions adopted in this study, the total internal leakage decreases as the radius is increased, improving the performance of the compressor, as can be confirmed through the results shown in Figs. 15-18. It should be mentioned that such behavior is not a rule and, as matter of fact, it depends on the compressor geometric parameters as well as the operating conditions.

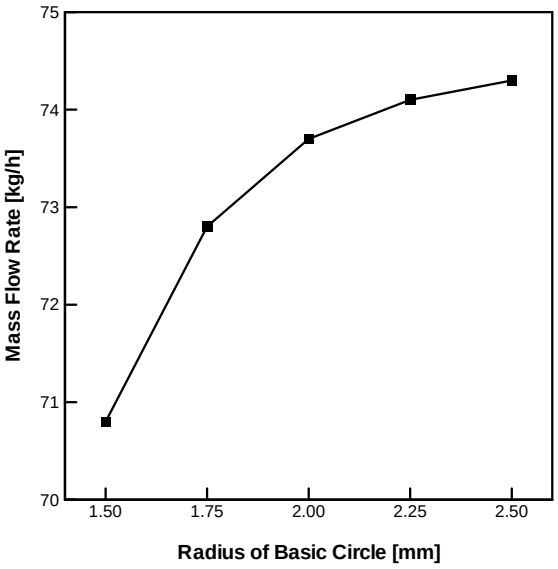

Figure 15. Influence of the basic circle radius on the mass flow rate.

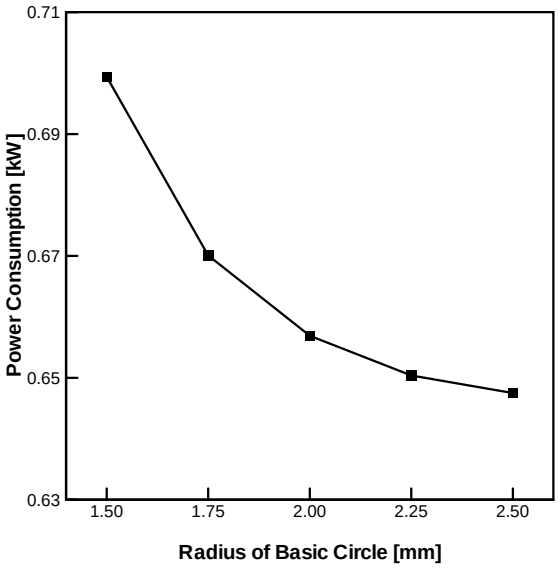

Figure 16. Influence of the basic circle radius on the power consumption.

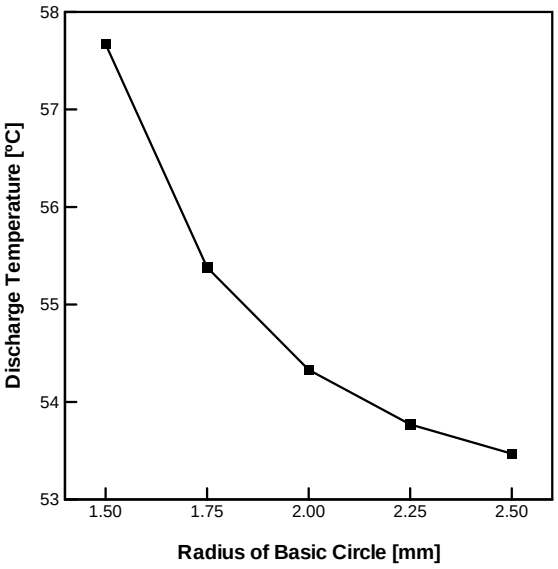

Figure 17. Influence of the basic circle radius on the discharge temperature.

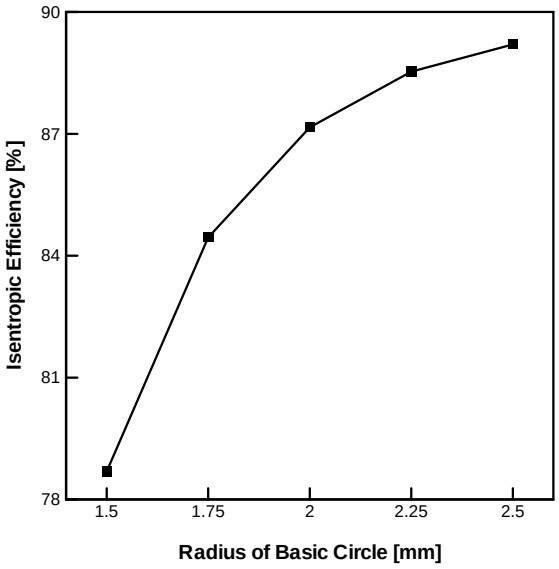

Figure 18. Influence of the basic circle radius on the isentropic efficiency.

4. CONCLUSIONS

This paper presented a numerical model to simulate the compression process in scroll compressors, which differs from the others in the literature as to the calculation of the chamber volumes and the solution procedure as well. The model was adopted to investigate the performance of scroll compressors subject to different operating conditions and also design changes. It was demonstrated the importance of discharge valves when the compressor runs at under compression conditions as well as the necessity of valves at intermediate positions in over compression situations. It was also observed the impact of leakages on the compressor performance, in which the top leakage is usually the most damaging for scroll compressors. At last, for the compressor and the operating conditions adopted in this study, the compressor performance was improved as the radius of basic circle was increased, although such behavior is not a rule.

5. ACKNOWLEDGEMENTS

The present study had the support from FINEP (Federal Agency of Research and Projects Financing), EMBRACO and CNPq (Brazilian Research Council).

6. REFERENCES

ASHRAE, 2004. “Handbook - heating, ventilating and air-conditioning systems and equipment”, ASHRAE Inc., Atlanta, USA.

Caillat, J.L., Ni, S. and Daniels, M., 1988, “A computer model for scroll compressors”, Proceedings of International Compressor Engineering Conference at Purdue University, pp. 47-553.

CARRIER CORPORATION, 2004, “Scroll compressors: high efficiency compression for commercial and industrial applications” New York, USA, 15 Nov. 2008, <http://www.xpedio.carrier.com/idc/groups/public/documents/marketing/811-20065.pdf.>

Chen, Y., Halm, N.P., Groll, E.A. and Braun, J.E, 2002, “Mathametical modeling of scroll compressors – part I: overall scroll compressor modeling”, Int. Journal of Refrigeration 25, pp. 731-750.

Creux, L., 1905, “Rotary Engine”, US Patent 801,182.

Ekelöf, J., 1933, “Rotary Pump or Compressor”, US Patent 1,906,142.

Gomes, A.R., 2006, “Análise comparativa de mecanismos de compressão para aplicação em refrigeração doméstica”, MSc. Thesis – Federal University of Santa Catarina, Department of Mechanical Engineering, in Portuguese.

Huang, Y., 1994, “Leakage calculation through clearances”, Proceedings of International Compressor Engineering Conference at Purdue University, pp. 35-40.

Morishita, E., Sugihara, M., Inaba, T., Nakamura, T. and Works, W., 1984, “Scroll compressor analytical model”, Proceedings of International Compressor Engineering Conference at Purdue University, pp. 487-495.

Nieter, J.J., 1988, “Dynamics of scroll suction process”, Proceedings of International Compressor Engineering Conference at Purdue University, pp. 165-174.

NIST, National Institute of Standards and Technology, 2008, “Refprop - Reference fluid thermodynamic and transport properties”, version 8, USA.

Suefuji, K., Shiibayashi, M. and Tojo, K., 1992, “Performance analysis of hermetic scroll compressor”, Proceedings of International Compressor Engineering Conference at Purdue University, pp. 75-84.

Tojo, K., Ikegawa, M., Maeda, N., Machida, S., Shiibayashi, M. and Uchikawa, N., 1986, “Computer modeling of scroll compressor with self adjusting back-pressure mechanism”, Proceedings of International Compressor Engineering Conference at Purdue University, pp. 872-886.

Wang, B., Li, X., Shi, W., 2005, “A general model of scroll compressors based on discretional initial angles of involute”, Int. Journal of Refrigeration, Vol. 28, pp. 958-966.

Yanagisawa, T., Cheng, M.C., Fukuta, M. and Shimizu, T., 1990, “Optimum operating pressure ratio for scroll compressor”, Proceedings of International Compressor Engineering Conference at Purdue University, pp. 425-433.

Zhenquan, L., Guirong, D., Shicai, Y., Mingzhi, W., 1992, “The graphic method of modified wrap of scroll compressor”, Proceedings of International Compressor Engineering Conference at Purdue University, pp. 1099-1106.

7. RESPONSIBILITY NOTICE

The authors are the only responsible for the printed material included in this paper.